

The phosphorus-31 spectra of dielectrophoretically reoriented tubules in the H_{II} phase of DOPE

Peter Osman ^{a,*}, Bruce Cornell ^b

^a CSIRO, Bradfield Rd., W. Lindfield, NSW 2070, Australia

^b CSIRO, Delhi Rd., N. Ryde, NSW 2070, Australia

Received 25 April 1995; revised 24 August 1995; accepted 19 September 1995

Abstract

³¹P electric field nuclear magnetic resonance measurements are described which assess the effect of electric field on the orientation of tubules comprising the H_{II} phase of dioleoylphosphatidylethanolamine. A model, based on dielectrophoretic effects, was used to predict that a field of 4 MV/m would change the orientation of the lipid tubules in a H_{II} phase. The excitation pulse was biphasic to help discriminate electric field interactions with free ions or permanent dipoles from interactions with induced dipoles, as well as to control the problems of ohmic heating, electrolysis and polarisation associated with dc or unbalanced ac excitation voltages. Spectra consistent with irreversible electrorotation and with reversible and transient electrorotation were observed. No response to the electric field was seen in certain cases. The conditions for irreversible and reversible electrorotation and failure to rotate have been tabulated and are discussed. Finally, some simple models are considered, in order to calculate the energies involved, if the observed NMR spectra are interpreted as arising from lipid H_{II} phase reorientations.

Keywords: NMR; Phospholipid; Inverted hexagonal (H_{II}) phase; Pulsed electric field

1. Introduction

The means by which electrical potentials interact with cell membranes and their constituents are not well understood. For example, such fields might influence membrane function through a mediating process such as the modulation of ion concentration, membrane thickness, or the conformation of lipidic structures. It is, therefore, of interest to measure conformational changes in lipid structures arising from externally applied electrical potentials.

Theories of the electric field dependence of membrane processes tend to discount dielectrophoretic effects, as being insignificant compared to first-order coulombic effects ([1,2] and references therein). However, electric field heterogeneity may occur in a bilayer membrane and the possibility of dielectrophoretic effects can therefore be considered.

Dielectrophoresis has been defined as the translational motion of neutral matter caused by polarization effects in a non uniform electric field [3]. For particles on the macro-

scopic scale such forces are clearly observable. However, the earliest consideration concluded that these forces would be negligible at the molecular level [1]. Subsequent work on the effect of non-uniform electric fields at the molecular level [4–10] showed that interactions occurred between such fields and macromolecular polymers of molecular mass as low as 600 kDa.

In recent years there has been an increase in the investigation of dielectrophoretic rotation in large biological structures such as yeast cells [11,12] and mammalian cells [13]. Similarly, a number of papers have dealt with the effect of electric field on macroscopic lipid structures. Most of these investigations have been electro-optical in nature with a significant level of work being carried out by optical microscopy, thus:

(i) Textural changes have been observed in hydrated lecithin with application of an electric field [14].

(ii) The application of electric field to vesicles has been shown to elongate them [15] or cause them to rotate [16–18].

(iii) Myelin figures [19] and phospholipid tubules [20] have been observed to change their orientation in response to the application of electric field. The square law relation-

* Corresponding author. Fax: +61 2 4137631.

ship between the time constant for orientation of myelin figures and electric field strength led to the suggestion that the mechanism for reorientation was charge separation and movement of the polar groups of the lipid molecules. Such a 'dielectrophoretic' interaction is also consistent with the evidence for reorientation of H_{II} tubules in the presence of a biphasically pulsed electric field. This is described below.

2. Materials and methods

The method used for obtaining spectra from lipid samples while applying electric field was similar to that described in a previous report [21].

2.1. Instrumentation

NMR measurements were made with a CXP300 spectrometer (Bruker, Karlsruhe, Germany), using a modified static solid state probe, type Z32DR with custom-made solenoids. A spin-locking pulse sequence, with proton decoupling, was used for the ^{31}P spectra. NMR spectra were acquired using a recycle time of 2 s, a sweep width of 62.5 kHz, line broadening of 200 Hz, and 90° pulses typically between 10 μs and 13 μs .

The electric field generator had a maximum output potential of 400 V and could be used asynchronously or synchronously with the NMR pulse programmer. The excitation was arranged to be a charge balanced biphasic, rectangular wave, which could be continuous or in the form of synchronised bursts. The number of pulses, their amplitude, repetition rate and duration, prior to the NMR 90° pulse, could be varied independently. The peak continuous power dissipation was 1 W. Sample spacers of 25 μm and 100 μm thickness were used so that nominal electric field strengths across the sample of between 4 MV/m to 16 MV/m were achievable.

Sample electrical impedance was measured before and after the NMR measurements, using impedance spectroscopy, sweeping from 1 kHz to 0.1 Hz (Associative Measurement, Sydney, Australia).

2.2. Sample preparation

The study was carried out using DOPE obtained from Avanti Polar Lipids (Alabaster, AL) and the lipid was used without further purification. The method of assembly followed the guidelines given in a previous report [22]. A single pair of slides, coated with gold electrodes, was used. The material for the 100 μm spacers was double-sided tape (Cat. 136-3M, Sydney, Australia), while for 25 μm spacings 920 'Scotch' adhesive transfer tape was used (GPA Industrial Supplies, Sydney, Australia).

The gold-coated microscope slides were assembled and 100 μl of 100 mg/ml DOPE in CHCl_3 was added to the centre of each slide, covering an area of approx. 25 mm^2 .

The samples were pumped under vacuum for about 12 h. The lipid on each slide was covered with a few microlitres of deionised water and the slides were placed in a saturated water vapour atmosphere at between 2°C and 4°C for up to 5 days, until the lipid samples appeared white and swollen and had remained in this state for at least a day. This was found to be the most reliable method for ensuring a uniform hydration of the H_{II} phase.

The 100 μm spacers were then applied and the second of the electrode pair was taped to the lipid coated slide, forming a slide pair. The sample area varied from about 5 mm^2 to 25 mm^2 . The smaller areas allowed well-hydrated samples of higher impedance so that the generator could produce pulses of greater electric field strength, but at the cost of NMR sensitivity. The surplus lipid material was gently squeezed out of the slides. The remaining lipid was then allowed to equilibrate at 100% relative humidity, under nitrogen, at room temperature for 24 h.

At this point, when well-hydrated samples were required, the slides were assembled into 5 mm diameter NMR tubes each containing a sponge saturated with deionised water. Other samples without excess water were assembled into NMR tubes without a saturated sponge. The electrical impedance was then measured in order to determine the maximum intensity of electric field which could be applied and to provide an indication of the degree of hydration of the lipid matrix. Both of these parameters were expected to affect the outcome of electrorotation experiments.

3. Results

3.1. Impedance spectroscopy

All samples were measured by impedance spectroscopy before and after acquiring the electric field NMR spectra. Fig. 1 shows typical impedance spectra for samples with free water, without excess water and partially dried. For electrorotation to occur it was necessary for the initial sample impedance to lie between A and B. Impedances in the region of A inhibited electrorotation until some degree of drying had occurred during application of electric field. For samples which were not kept at 100% relative humidity, the impedance was observed to alter during electric field NMR, probably due to heating effects and consequent drying of the lipid sample.

3.2. Line shapes for aligned and electrically reoriented H_{II} tubules

The chemical shift anisotropy for an array of aligned membranes in the H_{II} phase is given ([22] and references therein) as:

$$\left(\frac{\Delta\nu(\alpha)}{\nu_i(\alpha)} \right)_{H_{II}} = \frac{1}{3} \Delta\sigma_{L_a} \left(\frac{3\cos^2(\alpha) - 1}{2} \right) (\text{ppm}) H_{II} \quad (1)$$

This equation was used to model the spectral density functions of the NMR spectra reported here. Fig. 2 is a scheme, derived from Eq. (1), describing the H_{II} lipid phase and the orientation dependence of the corresponding magnetic resonance lines. The simulations attached to the spectra shown in this report are composites of these lines.

3.3. Planarised H_{II} tubules

The line shape for H_{II} tubules randomly oriented in two dimensions but restricted to a plane, is obtained from the superposition of lines, each derived from Eq. (1). Thus, if the normal to the plane is oriented at 90° to H_0 , the superposition of lines at all angles gives a catenary line shape (Fig. 2).

Fig. 3A and 3C show the 0° and 90° spectra for samples of DOPE which have been aligned between glass slides. Thus in 3A the normal to the plane of the slides is parallel to H_0 , i.e., at 0° ; while for 3C the slide normal is at right-angles to H_0 , i.e., the 90° case. The narrow line of spectrum A together with the catenary described by C were consistent with the alignment of the H_{II} tubules in the plane of the glass slides. It was observed that such samples, when kept at 100% relative humidity, had a relatively low proportion, if any, of aligned material, whereas samples which were partially dried, until their impedance corresponded to either Fig. 1B or 1C, showed a high degree of alignment.

3.4. Electrically oriented H_{II} tubules

Fig. 3 also compares spectra taken from planarised DOPE samples in the H_{II} phase with and without the application of electric field. A and C were taken without

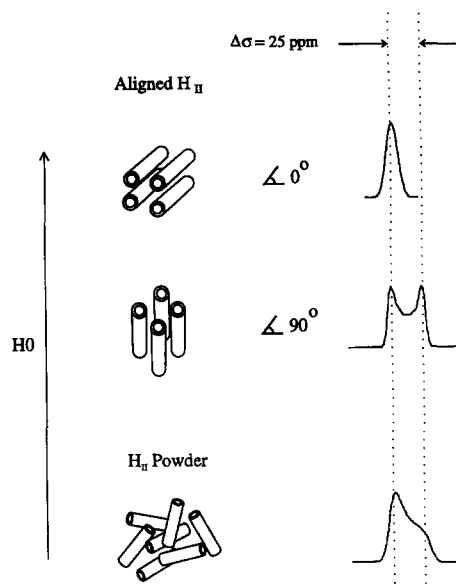


Fig. 2. A schema showing the lipid H_{II} phase and the orientation dependence of the corresponding NMR line shapes. The arrow labelled H_0 shows the direction of the magnetic field.

the electric field, while B and D were the corresponding 0° and 90° spectra for samples exposed to an electric field. Sample (i) was exposed to single pulses synchronised with the NMR 90° pulses, while sample (ii) was exposed to a continuous rectangular wave excitation. These spectra were consistent with an irreversible reorientation of approx. 50% of the H_{II} tubules by application of an electric field. They were simulated by the superposition of an H_{II} powder with 0° reoriented tubules. While such reorientations were regularly seen it was not unusual to observe instead a

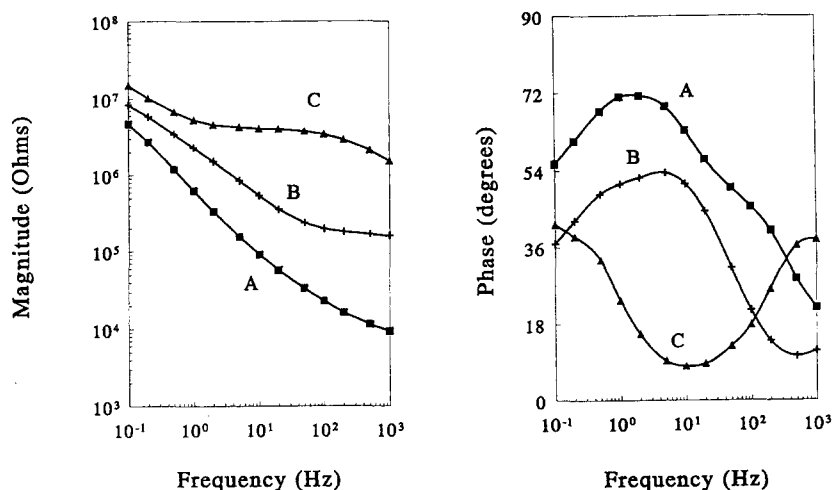


Fig. 1. Impedance spectra are shown above for a single DOPE NMR sample at different hydrations thus: (A) was assembled and stored at 100% relative humidity at 0.2°C for several days (i.e., in L_α phase); (B) was assembled at 100% relative humidity and dried at 65°C ; (C) was assembled at 100% relative humidity, dried at 65°C and stored with dry silica-gel. All spectra were taken at ambient temperature (i.e., in H_{II} phase). The spectral region between (A) and (B) is typical of viable initial conditions for samples to be dielectrophoretically rotated. The region of spectrum (B) corresponds to measurements made when samples were removed shortly after dielectrophoretic rotation.

reversible misalignment of the initially aligned spectrum in response to electric field.

3.5. Samples aligned with electric field

Fig. 4 shows a sequence of spectra taken from a planarised DOPE sample before, during and after application of an electric field. Fig. 4A shows the sample mechanically oriented with the normal to the plane of the slides at right-angles to H_0 , while 4B has the slide normal parallel to H_0 . The 7.5 ppm difference in chemical shift between A and B is an artefact, which is evident when the sample is mechanically rotated with respect to H_0 , because of its very small size and its dielectric anisotropy. The spectra show that the H_{II} tubules are aligned in the plane of the slide but with approximately 50% randomly oriented. Fig. 4C gives the spectra for the same orientation as B but with an electric field of 4 MV/m applied in 100 ms pulses prior to and synchronous with the free induction decay. A peak consistent with the process of irreversible electrorotation is evident at this stage. Fig. 4D and 4E give the line

shapes for the sample with the normal to its plane oriented respectively at right angles or parallel to H_0 . These spectra were obtained after the application of the 4 MV/m field and with 0 V applied to the sample. It can be seen that the composite and single peaks evident in 4A and 4B, at 90° and at 0° respectively, are now reversed with the composite peak being at 0° and the single peak at 90° . These spectra are consistent with electrorotation of approximately 40% of the tubules.

3.6. Samples reversibly and partially aligned with electric field

Fig. 5 shows two examples of reversible electrorotation which were subsequently followed by breakdown of the sample into a powder. The signals were weaker than the irreversibly rotated examples because of the limited number of free induction decays obtainable while the samples were in this transient state.

The first example demonstrates the reversibility of the

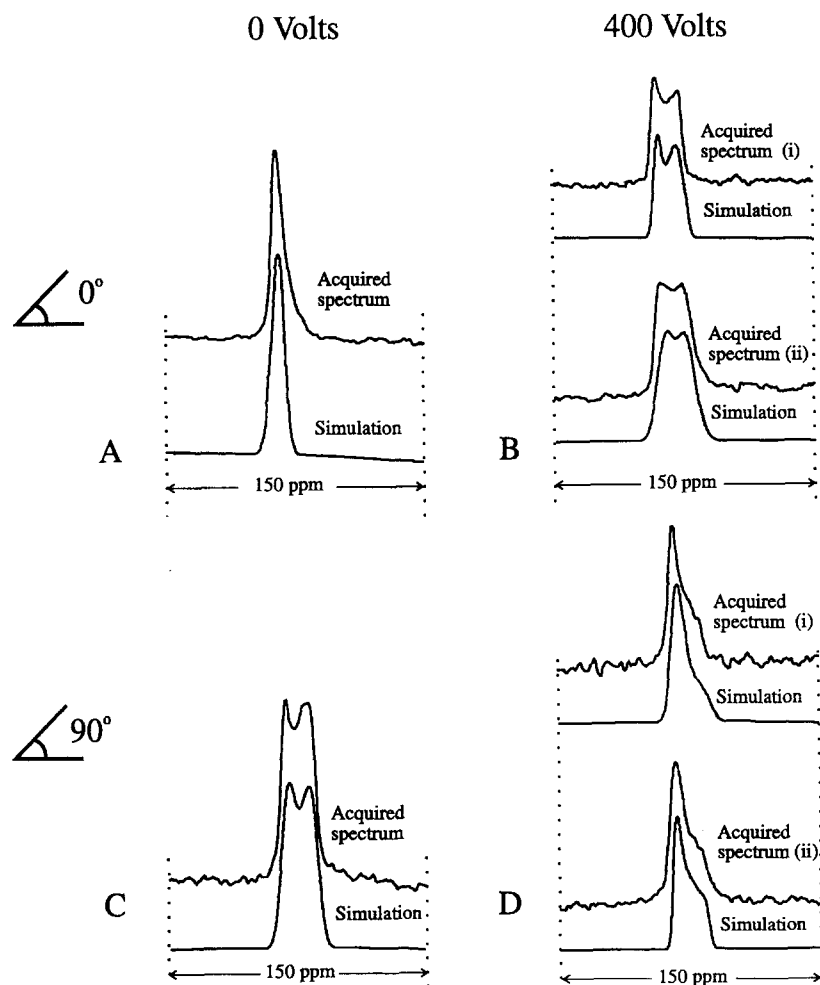


Fig. 3. The series of ^{31}P -NMR spectra shown above are consistent with dielectrophoretic rotation. Spectra (A) and (C) were taken before the application of electric field and show a single line at 0° and a catenary at 90° consistent with the alignment of tubules in the plane of the glass slides containing the sample. (B) and (D) show the 0° and 90° spectra for two similar samples which had been exposed to electric field. These spectra show a composite line at 0° consistent with the presence of both powdered and realigned H_{II} tubules. At 90° only the powdered component was visible.

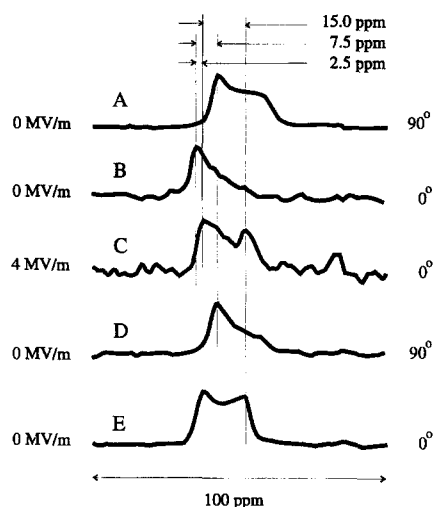


Fig. 4. A sequence of ^{31}P -NMR spectra taken from a planarised DOPE sample. Spectra were acquired with the slide normal either at 0° or at 90° to the magnetic field, H_0 . A single biphasic 4 MV/m pulse was progressively increased from 1 ms to 100 ms, at which point the spectral changes shown in (C), (D) and (E) were observed. The number of transients for each spectrum were respectively: 35K, 2.5K, 2.5K, 5K and 20K for (A), (B), (C), (D) and (E).

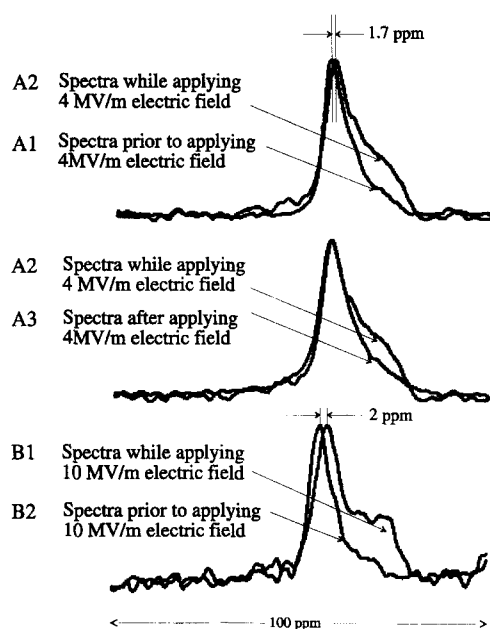


Fig. 5. This series of ^{31}P -NMR spectra shows partial and reversible dielectrophoretic movement of H_{II} tubules. (A1) to (A3) were acquired from a sample while subjecting it to 4 MV/m pulses (one pulse per NMR transient). These were progressively increased in duration from 0.1 to 20 ms. (A1) shows the spectrum prior to applying the electric field. At 20 ms a partial rotation was evident as a broadening in the spectrum (A2). The pulse width was not increased further and with removal of the electric field the spectrum reverted to its original line shape (A3). An irreversible 'upfield' chemical shift of 1.7 ppm was also observed. Spectra (B1) and (B2) were acquired from a sample, formed using a 25 μm spacer, to which a 10 MV/m pulse train of 3×20 ms pulses was applied. The line broadening and chemical shift were correspondingly greater. The number of transients acquired for (A) and (B), respectively, were 2.5K and 5K.

electrorotation. Spectrum A1 was obtained before applying an electric field and is overlaid on A2, which was obtained during application of a 4 MV/m field singly pulsed at 100 ms. The broader spectrum is indicative of an increase in alignment of H_{II} tubules in the direction of the electric field. Similarly spectrum A2 is overlaid on A3, which was acquired after the 4 MV/m, 100 ms synchronous pulse was removed. In this second comparison the spectrum without electric field has reverted to the narrower line width.

The second example shows spectra acquired before and during application of a field of 10 MV/m. In this case a triple 20 ms pulse was used prior to and synchronised with the free induction decay.

The chemical shift changes seen in samples A and B, were evident in all samples subjected to an electric field. The chemical shift differences lay between 1 and 2.5 ppm. They were correlated with both the field intensity and the field duration and were associated both with the transition from aligned to powder samples and with spectra showing the greatest degree of electrorotation, thus the spectra of Fig. 4C, 5A2 and 5B1 had chemical shift changes of 2.5 ppm, 1.7 ppm and 2 ppm respectively, in response to the electric field.

3.7. The effects of pulse width, electric field and time

Spectra A to E in Fig. 6 show the effect of pulse widths, varying from 1 ms to 100 ms, on a synchronously pulsed sample. It can be seen that there is no discernible effect at

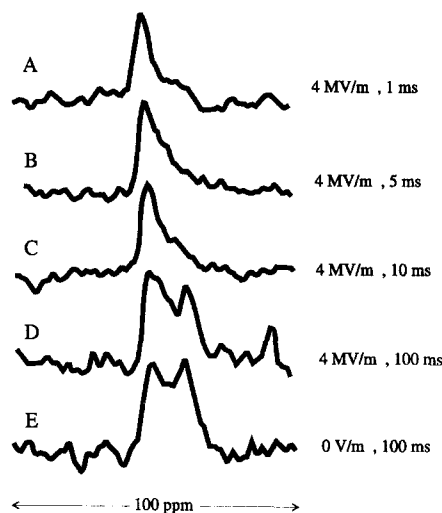


Fig. 6. The above series of ^{31}P -NMR spectra shows the onset of dielectrophoretic rotation as the electric field pulse width was increased. Spectra were acquired from a single sample under the same NMR conditions as for Fig. 4 and with the normal to the slide plane collinear with the magnetic field H_0 . A single biphasic 4 MV/m pulse was progressively increased from 1 ms to 100 ms, at which point the spectral changes shown in (D) were observed. Spectrum (E) was then acquired immediately after removal of the electric field excitation. The number of transients for each spectrum was 2500.

10 ms and below, while 100 ms pulses induce spectra consistent with dielectrophoretic rotation. These spectra were obtained at 4 MV/m. The final values determined for the single pulse width threshold were between 100 ms and 150 ms. Spectra indicative of transient dielectrophoretic rotation were also observed between 20 ms and 1 ms repetition periods for continuous rectangular wave electric fields. However, such experiments were harder to control because of ohmic heating and consequent drying of the sample.

The chemical shift appeared to be a sensitive indicator of potential dielectrophoresis. Fig. 7 shows that the ^{31}P chemical shift remains unchanged with pulse width until a value of 10 ms and then moves upfield with a final value at 100 ms of about 2 ppm. Values above 2.5 ppm were not observed during dielectrophoretic rotation. These shifts are consistent with an early disordering of H_{II} tubules which were initially aligned or partially aligned in the plane of the slides. The electric field threshold at which single pulses caused electrorotation was found to be between 3 MV/m and 4 MV/m for synchronous pulse bursts and between 2 and 3 MV/m for continuous pulsation. Fig. 7b shows the chemical shift to be a coarse indicator of the effect of electric field on the H_{II} tubules. In this instance the shift moved upfield as the electric field reached a threshold value prior to spectral changes consistent with H_{II} tubule rotation. It was observed, however, that simply increasing the field did not increase the probability that rotation would be observed. The evidence accumulated to date indicates that a band of values between 3 MV/m and 4 MV/m produces rotation, with excessive fields producing a powder spectrum.

3.8. The conditions for electrorotation

15 out of 25 measurements were found to be consistent with the dielectrophoretic rotation of H_{II} tubules. Table 1 summarises those parameters which appeared to affect the ability of the sample to exhibit such rotation. Some general observations can be made:

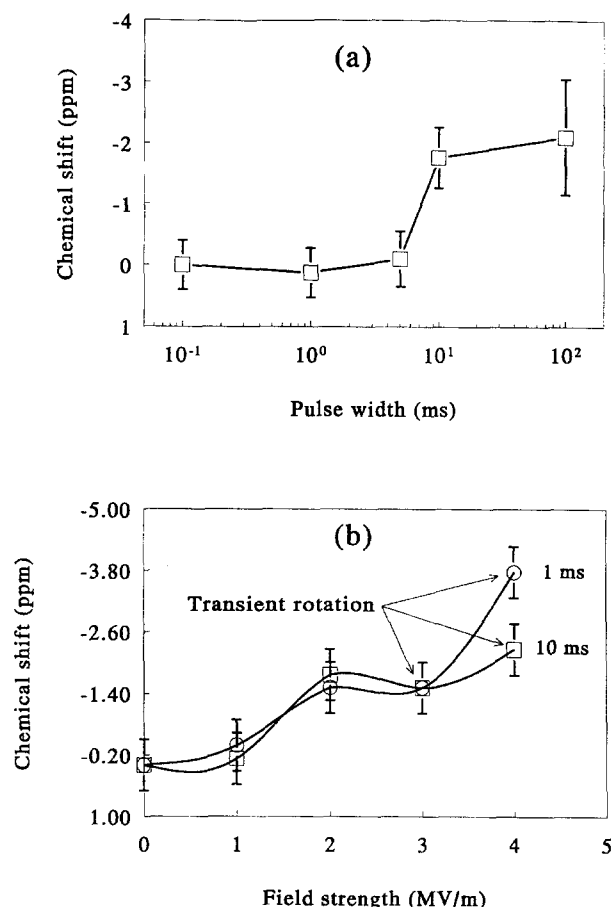


Fig. 7. These graphs were taken from spectra whose electrorotation properties are summarised in Table 1. The apparent change in ^{31}P chemical shift of the aligned H_{II} tubule lines as a function of (a) pulse width and (b) field strength is given. These changes were observed as a result of alterations in the spectrum consistent with transient realignment of the H_{II} tubules. Such changes were also observed when the sample became powdered.

(1) Where samples failed to electrorotate, only those parameters have been recorded which were varied during the first 20 000 free induction decays with electric field. Attempts made to electrorotate the sample after this num-

Table 1

A summary of the conditions for irreversible and reversible electrorotation and for no electrorotation

	Irreversible electrorotation	Reversible transient electrorotation	No electrorotation
Pulse amplitude (MV/m)	3 to 4	3 to 10	4 to 12
Synchronised single pulse width (ms)	100 to 150	20 to 100	1 to 100
Synchronous multiple pulse width (ms)	n/a	5000 pulse trains of $3 \times \pm 20$ ms each	2500 pulse trains 3×0.1 ms to 3×20 ms
Asynchronous pulse repetition frequency (Hz)	50	100 to 1000	18 to 10000
Number of pulses prior to and during electro-rotation	10 000 to 14 251	4000 to 20 000	n/a
Sample thickness (μm)	100	25 & 100	100
Initial impedance at 1 kHz ($\text{k}\Omega$)	20 to 250	12 to 318	12 to 2500
Initial impedance transition frequency (Hz)	10 to 200	10 to 1000	40 to > 1000
Environmental humidity	Ambient or 100%	Ambient or 100%	Ambient, with silica gel or 100% rh
Number of samples	5	10	10

ber of electric field transients failed, probably due to irreversible changes to the sample structure, in particular, loss of alignment and dehydration. This was supported by the observation of increases in the sample impedance, indicating drying and reduction in relaxation as measured by $T_{1\rho}$, indicating reduced mobility in the H_{II} tubules.

(2) Dielectrophoretic rotation of H_{II} tubules was observed to occur in samples in which the initial impedance spectra lay between the values given in A and B of Fig. 3. Samples with greater impedances e.g., C were not observed to rotate. The increase in impedance was associated with a change in $T_{1\rho}$ from greater than 30 ms down to 10 ms, indicating a reduced mobility.

(3) Dielectrophoretic rotation, if observed, always occurred within the first 10 000 scans during which electric field was applied. It did not occur immediately. This was believed to be due to an increase in impedance of the sample with time as excess water was removed from gross leakage paths. The increase in impedance was confirmed by removing some of the samples after electrorotation had occurred. Values for such impedances were typically within 20% of those shown in Fig. 1B. These intermediate values of impedance allowed the voltage across the sample to increase, as the power limiter in the pulse generator switched off with the increase in sample impedance.

(4) Irreversible electrorotation was observed with both synchronous and asynchronous excitation, and when both modalities used field strengths between 3 MV/m and 4 MV/m. Synchronous single pulse excitation required pulse widths between 100 ms and 150 ms, while continuous excitation was at a frequency of 50 Hz.

(5) Irreversible dielectrophoretic rotation was not observed in samples subjected to greater than 4 MV/m. Samples which had demonstrated such rotation reverted to spectra consistent with random orientation as the field strength was increased and, in the case of asynchronous excitation, as the repetition rate was reduced to below 50 Hz.

(6) Table 1 shows that transient electrorotation was observed over a broader range of experimental parameters than those recorded for irreversible electrorotation.

4. Discussion

4.1. A numerical model for electrorotation in tubules of the H_{II} phase

Inverted hexagonal tubules which make up the H_{II} phase of DOPE have a water core diameter of 3.6 nm and the lengths between defects in these tubules appear, from a visual inspection of freeze-fracture electron photomicrographs [23,24] to be at least as low as 250 nm.

Models for the dielectrophoretic rotation, suggested by the spectra in this paper, require the consideration of domains or clusters of tubules. We considered two models

representing two extremes of the variety of possible domain structures. These were (i) single tubules and (ii) spherical clusters of tubules. In each case the dielectrophoretic energy was balanced against energy loss due to viscous friction and due to the dislocation of the tubule ends at the domain boundaries. The maximum and minimum energy losses due to viscosity effects are represented by the single tubule and the spherical domains, respectively. Thus, the electrostatic enthalpy for the rotation of each domain can be calculated as:

$$U = -\frac{\epsilon_0}{2} \int (\epsilon_w - \epsilon_l) [(E_{\parallel} - E_{\perp}) \cdot E_0] dV \quad (2)$$

Where U is the enthalpy, V is the sample volume, ϵ_0 represents the permittivity of free space, with ϵ_l and ϵ_w representing the relative permittivities of the lipid and water environment, respectively. E_0 is the externally applied field and E_{\perp} and E_{\parallel} are the field distributions within the sample, with the tubules aligned with the field and orthogonal to the field, respectively. Rewriting Eq. (2) for a single tubule and taking two additional terms, due to the viscosity (η) and the tubule end dislocation energy $G1$, into account, gives the free energy for dielectrophoretic rotation of an H_{II} tubule as:

$$G_{\text{tubule}} = \frac{\pi \cdot \epsilon_0 \cdot E_0^2 \cdot L \cdot a^2}{2 \cdot (kT)} \cdot \frac{(\epsilon_w - \epsilon_l)^2}{(\epsilon_w + \epsilon_l)} - \frac{\eta \cdot (\pi L)^3}{8 \cdot (kT) \cdot \tau} - \frac{G1}{(kT) \cdot N_A} \quad (3)$$

while for the case of the spherical domain the free energy can be expressed as:

$$G_{\text{sphere}} = \frac{\pi \cdot \epsilon_0 \cdot E_0^2 \cdot L_{\text{tot}} \cdot a^2}{2 \cdot (kT)} \cdot \frac{(\epsilon_w - \epsilon_l)^2}{(\epsilon_w + \epsilon_l)} - \frac{\eta \cdot \pi^3 D^4}{8 \cdot (kT) \cdot \tau \cdot b} - \frac{G1}{(kT) \cdot N_A} \cdot \frac{L^2}{b^2} \quad (4)$$

where L is the single tubule length and L_{tot} is the sum of the lengths of all the tubules in the sphere; D is the diameter of each of the spherical domains; τ is the period of the electric field pulse; a is the radius of the water core of the H_{II} tubules, b is their periodicity which is approximately equal to their outer diameter; and $G1$ is the molar energy required to dislocate a tubule at the domain boundary [25].

Fig. 8E and F predict the variation of the free energy in the spherical domain model for the experimental conditions described above with Fig. 8F showing that the dielectrophoretic rotation becomes unlikely for domains greater than 0.5 μm diameter and with tubule dislocation energies of greater than 0.18 kcal/mol. For the single tubule case (curves C and D) the free energy is not significantly greater than kT . Thus, it is more likely that clusters of tubules acted cooperatively to produce the experimental results observed.

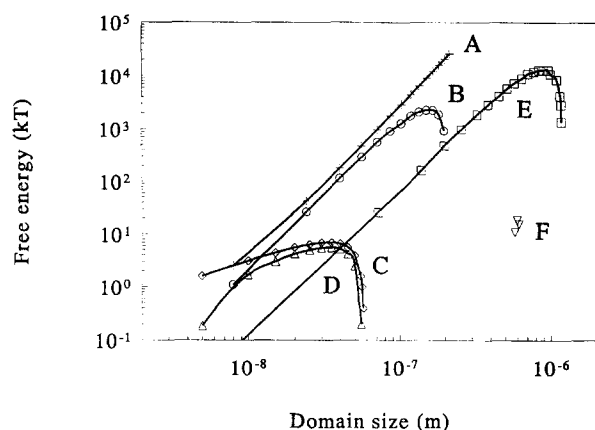


Fig. 8. Two models for dielectrophoretic rotation in H_{II} phase tubules are given for (i) spherical domains and (ii) single tubules. These describe the energy balance between dielectrophoresis, viscosity and the energy required to dislocate H_{II} tubules at the domain boundaries, (reference Eqs. (2)–(4)). (A) is calculated for the case of a spherical domain subject to 20 MV/m, 1 ms electric field pulses (typical of physiological action potentials); without accounting for viscosity effects. (B) is identical to (A) except that viscosity effects are included. (C) and (D) are single tubules subject to 20 MV/m, 1 ms pulses, respectively with and without the inclusion of tubule dislocation effects. (E) and (F) are spherical domains subject to 3 MV/m, 100 ms pulses (typical of the reported experimental conditions) excluding and including tubule dislocation effects respectively. Single tubules were not included for the 3 MV/m case as the free energy was always positive. Viscosity was taken as 1 poise and the tubule dislocation energy was taken as 3.4 kcal/mol, i.e., the maximum consistent with negative free energy for the reported experimental conditions.

It is of interest to note that voltage-dependent ion channels range in molecular mass from approximately 2 kDa (melittin – the active constituent in bee venom) to 2.3 MDa (a weakly voltage dependent, ryanodine receptor, calcium channel). Typically membrane ion channels such as potassium and sodium have molecular masses of about 200 kDa. During the action potential they are subject to changes in long-range electric field intensity of about 20 MV/m. Fig. 8A, B, C and D show calculations for the free energy when the derived value for tubule dislocation energy is applied to models subject to a change in electric field strength equivalent to that occurring during an action potential. The value corresponding to a cluster of tubules of 200 kDa is predicted from A and B as 8 kT when H_{II} tubule dislocation is accounted for and 15 kT when it is ignored. The field intensification for a model channel has been measured as having a value of between $\times 5$ and $\times 10$ [26]. The model geometry suggests that cooperative dielectrophoretic movement in an ion channel may be a significant contribution to the electric field interaction with voltage-dependent ion channels.

5. Conclusions

The conclusions and observations drawn from this series of measurements fall into three categories: (i) the use

of NMR techniques to observe the response of lipid dispersions to electric fields; (ii) the conditions for H_{II} tubules to reorient in the presence of an electric field; (iii) the development of models for dielectrophoretic rotation, to calculate the energies involved if the observed spectra were interpreted as lipid H_{II} phase domain reorientations.

Inspection of 15 out of 25 ^{31}P spectra from DOPE lipid samples in the H_{II} phase, before and after applying electric field, were consistent with the reorientation of aligned H_{II} tubules towards the direction of the electric field. Two classes of response were observed: transient and irreversible. The irreversible response provided the clearest indication of a 90° rotation and typically affected up to 50% of the sample. The reversible response affected approximately 10% to 20% of the mass of the samples in which it was observed. Additionally, the apparent movement appeared to be spread over a range of angles from 0° to 90° in both the reversible and irreversible cases. The observed movement provided evidence for dielectrophoretic interactions because of the biphasic nature of the excitation pulse between these small lipid-water structures and the applied electric field, and also because the rotational response occurred over a range of pulse widths including periods as short as 1 ms.

The range of field intensities for irreversible rotations was from 3 MV/m to 4 MV/m. Single pulse durations were from 100 ms to 140 ms and continuous pulse repetition periods were set at 20 ms. Transient dielectrophoretic reorientation was more frequently observed than the irreversible event. The range of field strengths for such changes was from 3 MV/m to 10 MV/m. The duration of the pulses lay in the range from 20 ms to 100 ms for single pulses and from 1 ms to 20 ms for continuous pulsing. Fig. 8 indicates that one reason, for the samples that did not reorient either transiently or irreversibly, may have been differences in the size of H_{II} domains between samples. Thus, domain sizes greater than $0.4\ \mu\text{m}$ would not have been expected to be affected by dielectrophoresis.

The dielectrophoretic energies involved in the reorientations described above were estimated to range from less than 1 kT for single tubules of any length, to 20 kT for 500 nm spherical domains of tubules acting cooperatively. The irreversible reorientations were more likely to have involved relatively large domains while the reversible events may have involved smaller domains i.e., lesser degrees of cooperativity.

These results suggest that dielectrophoresis may have a role in membrane processes and that it may be practical to observe electrically induced changes in ion channel conformation by NMR spectroscopy.

Acknowledgements

We gratefully acknowledge Dr. Frances Separovic for her many helpful comments and discussions and also the

support of the Cooperative Research Centre for Molecular Engineering and Technology which has provided access to the NMR facilities used in this paper.

References

- [1] Muller, F.H. (1938) ETZ. 59, Oct. 1155–1158. Nov. 1176–1182.
- [2] Tsong, T.Y. and Astumian, R.D. (1987) Prog. Biophys. Mol. Biol. 50, 1–45.
- [3] Pohl, H.A. (1951) J. Appl. Phys. 22, 869–871.
- [4] Debye, P.J.W., Debye, P.P., Eckstein, B.H., Barber, W.A. and Arquette, G.J. (1954) J. Chem. Phys. 22, 152–153.
- [5] Losche, A. and Hultschig, H. (1955) Kolloid Z. 141, 177–180.
- [6] O'Konski, C.T. and Haltner, A.J. (1957) Department of Chemistry, University of California, Berkeley, 79, 5634–5649.
- [7] Tinoco Jr, I. and Yamaoka, K. (1959) Department of Chemistry, University of California, Berkeley, 63, 423–427.
- [8] O'Konskii, C.T., Yoshioka, K. and Ortung, W.H. (1959) Phys. Chem. 63, 1558–1565.
- [9] Charney, E. and Yamaoka, K. (1982) Biochemistry 21, 834–842.
- [10] Yamaoka, K. and Fukudome, K. (1990) J. Phys. Chem. 94, 6896–6903.
- [11] Huang, Y. and Pethig, R. (1991) Meas. Sci. Technol. 2, 1142–1146.
- [12] Egger, M. and Donath, E. (1991) Bioelectrochem. Bioenerg. 26, 383–393.
- [13] Gascoyne, P.R.C., Huang, Y., Pethig, R., Vykoukal, J. (1992) Meas. Sci. Technol. 3, 439–445.
- [14] Val'kov, S.V. and Chumakova, S.P. (1982) Sov. Phys. Crystallogr. 26(7), 718–719.
- [15] Zeks, B., Svetina, S. and Pastushenko, V. (1990) Studia Biophys. 138(1–2), 137–142.
- [16] Hub, H.-H., Ringsdorf, H. and Zimmermann, U. (1982) Angew. Chem. Int. Ed. Engl. 21(2), 134–135.
- [17] Sevesk, F., Sukharev, S., Svetina, S. and Zeks, B. (1990) Studia Biophys. 138(1–2), 143–146.
- [18] Winterhalter, M. and Helfrich, W. (1987) Rapid Commun. Phys. Rev. A 36(12), 5874–5876.
- [19] Mishima, K. and Morimoto, T. (1989) Biochim. Biophys. Acta 985, 351–354.
- [20] Li, Z., Rosenblatt, C., Yager, P. and Schoen, P.E. (1988) Biophys. J. 54, 289–294.
- [21] Osman, P. and Cornell, B. (1994) Biochim. Biophys. Acta 1195, 197–204.
- [22] Mehring, M. (1976) in NMR Spectroscopy in Solids (Diehl, P. and Fluck, E., eds.), Springer, Berlin.
- [23] Borovjagin, V.L., Vergara, J.A. and McIntosh, T.J. (1982) J. Membr. Biol. 69, 199–212.
- [24] Webb, M.S., Hui, S.W. and Steponkus, P.L. (1993) Biochim. Biophys. Acta 1145, 93–104.
- [25] Tanford, C. (1973, 1980) in The Hydrophobic Effect, John Wiley, New York.
- [26] Bodrova, N.B. and Pasechnik, V.I. (1985) Biophysics 30(2), 285–290.